Panyim, S., & Chalkley, R. (1969) *Biochemistry 8*, 3972–3986.
Peacock, A. C., & Dingman, C. W. (1967) *Biochemistry 6*, 1818–1827.
Rabbani, A., Goodwin, G. G., & Johns, E. W. (1978) *Biochem. J. 173*, 497–505.
Rabbani, A., Goodwin, G. H., Walker, J. M., Brown, E., & Johns, E. W. (1980) *FEBS Lett. 109*, 294–298.
Renart, J., Reiser, J., & Start, G. R. (1979) *Proc. Natl. Acad. Sci. U.S.A. 76*, 3116–3120.
Romani, M., Rodman, T. C., Vidali, G., & Bustin, M. (1979) *J. Biol. Chem. 254*, 2918–2922.
Romani, M., Vidali, G., Tahourdin, C. S. M., & Bustin, M. (1980) *J. Biol. Chem. 255*, 468–474.
Rungger, D., Rungger-Brandle, E., Chaponnier, C., & Gabbiani, G. (1979) *Nature (London) 282*, 320–321.
Scheer, U., Sommerville, J., & Bustin, M. (1979) *J. Cell Sci. 40*, 1–20.
Spiker, S., Mardian, J. K. W., & Isenberg, I. (1978) *Biochem. Biophys. Res. Commun. 82*, 129–135.
Walker, J. M., & Johns, E. W. (1980) *Biochem. J. 185*, 383–386.
Walker, J. M., Hastings, J. R. B., & Johns, E. W. (1977) *Eur. J. Biochem. 76*, 461–468.
Weisbrod, S., & Weintraub, H. (1979) *Proc. Natl. Acad. Sci. U.S.A. 76*, 630–634.
Weisbrod, S., Groudine, M., & Weintraub, H. (1980) *Cell 19*, 289–301.
Whitlock, J. P., Jr., & Simpson, R. T. (1976) *Nucleic Acids Res. 3*, 2255–2266.

High-Potential Iron–Sulfur Proteins and Their Possible Site of Electron Transfer†

George Aprahamian and Benjamin A. Feinberg*

ABSTRACT: The electron-transfer mechanism of the Fe_4S_4* high-potential iron–sulfur proteins (HiPIP's) was explored via a stopped-flow spectrophotometric kinetic study of the reduction of *Chromatium vinosum* and *Rhodopseudomonas gelatinosa* HiPIP's by both native and trinitrophenyllysine-13 horse cytochrome *c*. The influence of electrostatic effects was also effectively partitioned from the redox process per se. The corrected rates were 12.3×10^4 and 3.8×10^4 M^{-1} s^{-1} for native with *C. vinosum* and *R. gelatinosa* HiPIP, respectively, and 17.5×10^4 and 5.46×10^4 M^{-1} s^{-1} for TNP-cytochrome *c* with the two HiPIP's, respectively. The faster rates of TNP-cytochrome *c* with the HiPIP's are unexpected in terms of possible steric interaction since lysine-13 is at the top of the heme crevice. In understanding the somewhat faster rates of the TNP-cytochrome *c* over native cytochrome *c* it is possible that (1) TNP-cytochrome *c* reacts more quickly since modification of the lysine-13 residue destabilizes somewhat the heme crevice or (2) in light of the hydrophobic nature of the trinitrophenyl group and the X-ray crystallographic structure of HiPIP, the TNP group facilitates electron transfer by interacting with a hydrophobic region on the HiPIP molecular surface. The region about the S*4 sulfur atom is the most exposed and accessible hydrophobic region on the HiPIP surface, in addition to being the point of closest approach of the S*4 to the external environment.

Much effort has been expended in the past decade in the determination of the oxidation–reduction mechanisms of the important classes of redox proteins, including the cytochromes *c*, flavoproteins, copper, and iron–sulfur proteins. Besides the study of the biological redox couples, redox protein mechanism has also been approached via the nonphysiological study of small molecule–protein reactions and to a much lesser extent biologically nonspecific protein–protein reactions. Nonspecific protein–protein redox reactions, however, are of particular interest since they ensure with much greater certainty that an outer-sphere electron-transfer mechanism will prevail (most probable for biological protein–protein reactions) and, for this reason, also mimic more closely the biological protein–protein reactions than the small molecule–protein reactions.

In this study the electron-transfer mechanism of the high-potential iron–sulfur proteins (HiPIP's)[1] is explored via a stopped-flow spectrophotometric kinetic study of the reduction of *Chromatium vinosum* and *Rhodopseudomonas gelatinosa* HiPIP's by both native and trinitrophenyllysine-13 horse cytochrome *c*. The TNP group is both particularly bulky and hydrophobic, and modification of the lysine-13 residue provides an especially interesting derivative of cytochrome *c* since it might be expected to partially block the heme crevice region where electron transfer is generally demonstrated to take place. Additionally, when lysine-13 is TNP modified, it does not transfer electrons to cytochrome *c* oxidase since the specific binding between the two molecules is disrupted (Smith et al., 1977; Ferguson-Miller et al., 1978). Lastly, in this work the electrostatic contributions to the redox rates have been effectively partitioned from the electron-transfer process per se to obtain electrostatically corrected rate constants. The need and usefullness of such corrections have been demonstrated (Feinberg & Johnson, 1980; Ilan et al., 1979); moreover, such corrections provide a clearer view of the HiPIP electron-transfer mechanism.

† From the Department of Chemistry and The Laboratory for Molecular Biomedical Research (Contribution No. 117), The University of Wisconsin—Milwaukee, Milwaukee, Wisconsin 53201. *Received June 30, 1980.* This work was performed with the support of the Science and Education Administration of the U.S. Department of Agriculture under Grant No. 5901-0410-8-0156-0 from the Competitive Research Grants Office, The Research Corporation, and The University of Wisconsin—Milwaukee Graduate School Research Committee.

[1] Abbreviations used: HiPIP, high-potential iron–sulfur protein; TNP, trinitrophenyl; Tris, 2-amino-2-(hydroxymethyl)-1,3-propanediol; phen, phenanthroline.

0006-2960/81/0420-0915$01.00/0

Experimental Procedures

Potassium ferricyanide and sodium dithionite were obtained from Fisher Scientific Co. Tris and Tris-HCl were obtained from Sigma Chemical Co., as was horse cytochrome *c*, Grade VI. The horse heart cytochrome *c* was purified by carboxymethylcellulose chromatography as described by Brautigan et al. (1978). Highly purified trinitrophenyllysine-13 cytochrome *c* (TNP-cytochrome *c*) was prepared by the method of Wada & Okunuki (1969) as modified by Osheroff et al. (1980). All other chemicals used were of reagent grade, and only double-distilled water was used.

Chromatium vinosum (pI' = 3.68) and *Rhodopseudomonas gelatinosa* (pI' = 9.50) HiPIP's were isolated and purified as described by Bartsch (1971, 1978), Tedro (1976), and De Klerk (1966). For the kinetic experiments extinction coefficients determined by Dus (1967) were used: 41.3 and 16.1 mM for reduced HiPIP at 283 and 388 nm, respectively; 39.3 and 21.8 mM for oxidized HiPIP at 283 and 325 nm, respectively. The extinction coefficient reported by Kortüm (1962) of 742.4 M^{-1} at 436 nm was used for ferricyanide.

Stopped-Flow Spectrophotometric Kinetics. Kinetic studies were carried out with a Durrum stopped-flow spectrophotometer with a pneumatic air-actuated pushing device. Absorption measurements were made with a linear optical configuration utilizing a tungsten lamp source and 2-cm light path. Phototube voltages were stored in a Northern Scientific NS-560 time-averaging computer modified to collect data at two scanning speeds in each of two 1024 memory cell storage units. The data were then hard copy plotted with a Houston Instruments Omnigraphic 2000 X-Y Recorder. Data were treated by a regression analysis of the linear form of the first-order rate law. Second-order rates were determined under pseudo-first-order conditions by using a series of increasing ferricyanide or protein concentrations.

Protein samples were taken from liquid nitrogen storage and thawed. An aliquot was taken and added to 1 drop of buffer containing <1 mg of dithionite or ferricyanide to obtain reduced or oxidized protein, respectively. For TNP-lysine-13 cytochrome *c*, ascorbate was used as reductant, since dithionite can reduce nitro groups to amino groups (Sokolvsky et al., 1967). The protein sample was passed over a small Sephadex G-25 column previously equilibrated with deoxygenated reaction buffer. The sample was caught in a stoppered glass vial, diluted with deoxygenated reaction buffer to get the desired concentration, and then loaded into the stop-flow syringe. The background buffer was 5.0 mM phosphate, and the ionic strength was further adjusted with sodium chloride. The reactions between the HiPIP's and ferricyanide were monitored at 500 nm, while the reactions between the HiPIP's and the cytochromes were monitored at 504 nm. The value of 500 nm is close to the maximum difference between oxidized and reduced HiPIP absorbance and 504 nm is an isobestic point for cytochrome *c*.

Electrostatic Corrections. The kinetic–ionic strength data were analyzed by a nonlinear least-squares regression analysis of eq 1 derived by Wherland & Gray (1976) from the Marcus theory of outer-sphere electron-transfer reactions and Debye potential theory:

$$\ln k_I = \ln k_\infty - 3.576\left(\frac{e^{-\kappa R_A}}{1+\kappa R_B} + \frac{e^{-\kappa R_B}}{1+\kappa R_A}\right)\left(\frac{Z_A Z_B}{R_A + R_B}\right) \quad (1)$$

where k_I is the observed rate constant at ionic strength I (M), Z_A and Z_B are the net charges of the reactants A and B, respectively, R_A and R_B are the radii of the reactants, A and B, $\kappa = 0.329I^{1/2}$ Å^{-1}, and k_∞ is the rate constant at infinite ionic strength (i.e., the rate that is independent of electrostatic interactions since the charges of reactants are fully shielded from each other by the ions of the electrolyte solution). The rate constant at infinite ionic strength is the electrostatically corrected rate constant, k_∞. From the curve fit both the apparent net charge of the protein and k_∞ are obtained. The predicted redox protein charge from eq 1 was compared to the net charge of the protein as determined from the sequence and cluster (Z_{seq}) at a particular pH. In this work all reactions were examined at pH 7.0. The radius of $Fe(CN)_6^{3-}$ was assumed to be 4.5 Å, and the radius of the protein was estimated from eq 2 (Tanford, 1961) where M_r = molecular weight. Equation 2 gives radii of 14.3, 15.1, and 16.6 Å for *R. gelatinosa* HiPIP, *C. vinosum* HiPIP, and cytochrome *c*, respectively. Each reaction was done in triplicate and investigated under pseudo-first-order conditions for HiPIP and at several ionic strengths in order to obtain electrostatically corrected rates.

$$R = 0.717M_r^{1/3} \quad (2)$$

Table I: Second-Order Rate Constants for Oxidation of HiPIP by Ferricyanide, pH 7.0, at Different Ionic Strengths

R. gelatinosa		*C. vinosum*	
I	k (M^{-1} s^{-1} × 10^{-4})	I	k (M^{-1} s^{-1} × 10^{-3})
0.009	10.34	0.009	0.55
0.024	7.32	0.034	1.22
0.039	6.01	0.059	1.68
0.059	5.35	0.109	2.41
0.109	4.39	0.159	3.05

Table II: Second-Order Rate Constants for Reduction of *R. gelatinosa* HiPIP by Native and TNP-cytochrome *c*, pH 7.0, at Different Ionic Strengths

native cyt *c*		TNP-cyt *c*	
I	k (M^{-1} s^{-1} × 10^{-4})	I	k (M^{-1} s^{-1} × 10^{-4})
0.009	1.1	0.009	2.0
0.019	1.3	0.024	2.6
0.039	1.7	0.046	3.2
0.059	2.1	0.079	4.2
0.109	2.5	0.109	4.6
0.209	3.6		

Table III: Second-Order Rate Constants for Reduction of *C. vinosum* HiPIP by Native and TNP-cytochrome *c*, pH 7.0, at Different Ionic Strengths

native cyt *c*		TNP-cyt *c*	
I	k (M^{-1} s^{-1} × 10^{-5})	I	k (M^{-1} s^{-1} × 10^{-5})
0.009	3.0	0.009	3.3
0.034	2.0	0.024	2.6
0.059	1.8	0.054	2.4
0.084	1.6	0.109	1.8
0.109	1.2		

Results

The kinetics for the oxidation of *C. vinosum* and *R. gelatinosa* HiPIP's by ferricyanide as well as their reduction by horse heart cytochrome *c* and trinitrophenyllysine-13 cytochrome *c* were studied at different ionic strengths at pH 7.0. The results are summarized in Tables I–III. The best curve fits to eq 1 of all the rates of oxidation and reduction as a function of ionic strength are shown in Figures 1–3.

For the oxidation of the two HiPIP's by ferricyanide, the net protein charge predicted from eq 1 was found to be quite

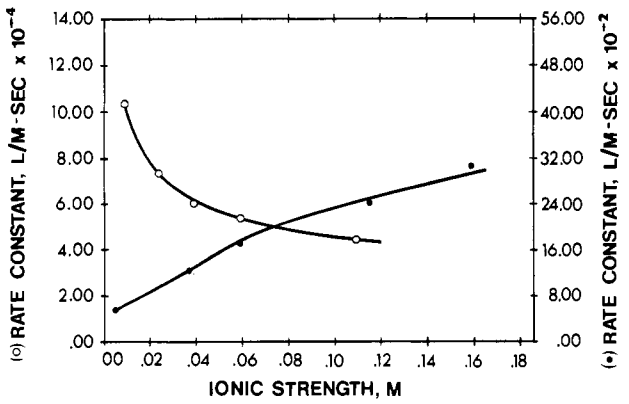

FIGURE 1: Rate of oxidation of *C. vinosum* HiPIP (●) and *R. gelatinosa* HiPIP (○) by ferricyanide as a function of ionic strength at pH 7.0. Solid lines are the best fit of eq 1 to the data.

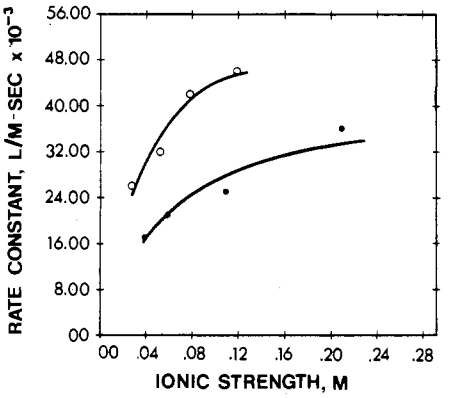

FIGURE 2: Rate of reduction of *R. gelatinosa* HiPIP by native (●) and trinitrophenyllysine-13 cytochrome *c* (○) as a function of ionic strength at pH 7.0. Solid lines are the best fit of eq 1 to data.

Table IV: Comparison of Z_{eq1} from Kinetic-Ionic Strength Data from Table I to Z_{seq}

	Z_{eq1}	Z_{seq}
R. gelatinosa	+1.9	+3.0
C. vinosum	−3.6	−3.0

close to the net protein charge obtained from the primary sequence of *C. vinosum* (Dus et al., 1973) and *R. gelatinosa* (Tedro et al., 1976, 1979) and the cluster, Z_{seq} (see Table IV). For the protein–protein redox reactions, the predicted charges of the cytochromes and the electrostatically corrected rates as calculated from the kinetic ionic strength experiments are summarized in Table V. For the charge of the HiPIP's, Z was taken to be Z_{seq}, since it can be concluded from Table IV that $Z_{eq1} \simeq Z_{seq}$ in the case of the HiPIP's (where $Z = -3$ for ferricyanide, $Fe(CN)_6^{3-}$).

Discussion

The best fit of the data for the reduction of *R. gelatinosa* HiPIP by ferricyanide yielded a charge on HiPIP of +1.9, which is in good agreement with the predicted charge of +3.0 (Z_{seq}) obtained from the primary structure. The charge calculated by eq 1 for *C. vinosum* HiPIP is −3.6, which is in very good agreement with the charge of −3 (Z_{seq}) predicted for reduced HiPIP from the primary structure. For the reduction of *C. vinosum* HiPIP by native cytochrome *c*, the best fit of the data yielded a charge of +5.1 for reduced cytochrome, which is in excellent agreement with the charge of 5.3 as determined from titration experiments (Matthew et al., 1978). The charge obtained for the trinitrophenyllysine-13 cytochrome *c* from the data for the reduction of *C. vinosum*

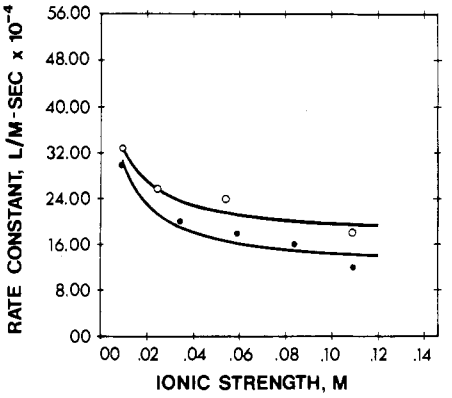

FIGURE 3: Rate of reduction of *C. vinosum* HiPIP by native (●) and trinitrophenyllysine-13 cytochrome (○) as a function of ionic strength. Solid lines are the best fit of eq 1 to the data.

HiPIP fit to eq 1 is 3.54. The difference in charge between the negative and modified cytochrome is 1.53, which is in good agreement with the loss of one positive charge upon modification of the lysine residue.

The data for the reduction of *R. gelatinosa* by cytochrome, when fit to eq 1, gave a charge on cytochrome of only +3.11 (vs. expected 5.3), and the data did not match the least-squares analysis especially well. This type of deviation has occurred in other ionic strength treatments and is discussed in a review of kinetic salt effects by Perlmutter-Hayman (1971). The experimental evidence seems to support his idea that, for reactions between ions of unlike sign, classical behavior is observed and the salt effect is governed by the principle of ionic strength (i.e., classical electrostatic interactions). On the other hand, for reactions between ions of like sign, the classical principle of ionic strength breaks down. Instead the rate is further influenced by the concentration of the supporting ion of opposite sign. In like-sign reactions small deviations occur when the background ion of the same sign as that of the two reacting species has a valency higher than one, whereas large deviations occur when the ion of opposite sign is polyvalent. In this work the reactions between *R. gelatinosa* HiPIP and the two cytochromes *c* are like-sign reactions, i.e., positive–positive, and the polyvalent phosphate ion (in the 5 mM background phosphate buffer) probably does contribute to the observed deviations. Support for this is found in the calculations based only on ionic strength–kinetic data at higher ionic strengths ($I > 0.24$) where sodium chloride has been used to increase ionic strength and is the main source of ionic strength; thus, there is relatively less polyvalent phosphate to cause deviation. In Table V are shown the results of the calculation done at the higher ionic strengths. Charges of 4.9 and 3.4 were obtained for native and TNP-cytochrome *c*, respectively, both values being in excellent agreement with the cytochrome charges of 5.1 and 3.5 for native and TNP-cytochrome *c* as obtained from the experiments with the oppositely charged *C. vinosum* HiPIP.

As noted earlier, the k_∞ calculated from eq 1 is the rate constant at infinite ionic strength, that is, it is an electrostatically corrected rate constant since the charge of the reactants are fully shielded from each other at infinite ionic strength. In Table V are summarized the k_∞ values for the four protein–protein reactions.

According to Marcus theory (Marcus, 1964), an increase in electron-transfer rate is expected as the potential difference in redox potential between the reactants increases; thus, the overall rate differences between the two HiPIP's are not surprising since the redox potentials of *C. vinosum* and *R. gelatinosa* HiPIP are 350–356 mV (Dus et al., 1967; Mizrahi

Table V: Electrostatically Corrected Rates and Predicted Cytochrome *c* Charge, Z_{eq1}, Compared to Charge Determined from Titration Studies, $Z_{titration}$[a]

reaction	Z_{eq1}	$Z_{titration}$	k_∞ (M^{-1} s^{-1} × 10^{-4})
cyt c_{red} + *C.v.*[e] $HiPIP_{ox}$	5.1	5.3	12.3
TNP-cyt c_{red} + *C.v.* $HiPIP_{ox}$	3.5	4.3[b]	17.5
cyt c_{red} + *R.g.*[f] $HiPIP_{ox}$	3.1 (4.9)[c]	5.3	3.24 (3.82)[d]
TNP-cyt *c* + *R.g.* $HiPIP_{ox}$	2.6 (3.40)[c]	4.3[b]	5.12 (5.46)[d]
C.v. HiPIP: k_∞(TNP)/k_∞(NAT) = 1.42			
R.g. HiPIP: k_∞(TNP)/k_∞(NAT) = 1.43			

[a] Matthew et al. (1978). [b] This is the charge of native cytochrome *c* at pH 7.0 − 1 since a single positive charge is lost after TNP modification. [c] The predicted cytochrome charges based upon the kinetic-ionic strength data at $I > 0.24$. [d] The predicted k_∞ based upon kinetic-ionic strength data at $I > 0.24$. [e] *C.v., Chromatium vinosum.* [f] *R.g., Rhodopseudomonas gelatinosa.*

et al., 1976) and 340 mV (Dus et al., 1967), respectively. Both native and TNP-cytochrome *c* have an E^0 = 272 mV as measured in Tris–acetate buffer (Osheroff, 1979). What is more surprising and of greater interest is that for both HiPIP's the rate of reaction with TNP-cytochrome *c* is ~1.4 times faster than with native cytochrome *c* (see Table V).

It was originally thought that the bulky TNP group, which blocks biological activity with cytochrome *c* oxidase, would in these nonphysiological reactions *sterically* block the heme crevice in its interaction with HiPIP; instead a small but systematic enhancement was observed. In the case of the TNP-cytochrome *c*–cytochrome *c* oxidase reaction, the TNP-cytochrome *c* is inactive because the *charge* of the lysine residue has been changed from positive to neutral, and, consequently, the electrostatic interaction of this lysine with cytochrome *c* oxidase is disrupted and specific binding is disrupted (Ferguson-Miller et al., 1978). Thus, in the case of the biological donor–acceptor pair, steric effects also apparently are not at issue.

When the origin of the enhanced rate of TNP-cytochrome *c* vs. native cytochrome *c* (for a given HiPIP) is considered, apparently neither redox potential differences nor heme crevice opening or disruption play a role, since at pH 7.0 the $E^{0\prime}$ is the same for TNP-cytochrome *c* and native cytochrome *c* and the 695-nm band is intact in TNP-cytochrome *c*. The maintenance of the 695-nm band in the TNP-cytochrome (and also the $E^{0\prime}$) indicates that the heme crevice has not been enlarged or opened because of the modification; however, it should be noted that the heme crevice is somewhat destabilized by the TNP modification since (Osheroff et al., 1980) the salt bridge between the ϵ-amino of the lysine-13 and the γ-carboxyl of glutamyl residue 90 (top of heme crevice) is disrupted. In this light, one possible reason that the TNP-cytochrome reacts faster with the HiPIP's is that while the heme edge is still intact, it is more flexible and possibly more exposed during its molecular "breathing". This relatively more exposed heme edge (as compared to native cytochrome *c*) then reacts with some region on the HiPIP molecular surface.

An alternative and not mutually exclusive mechanism is that the heme edge of the TNP-cytochrome *c* is indeed more hydrophobic precisely because of the TNP modification and that the more hydrophobic TNP–heme edge interacts with a specific hydrophobic region on the HiPIP surface. Although this mechanism is speculative, there is some evidence for it to be found in the examination of the sequence data and X-ray crystallographic structure of HiPIP.

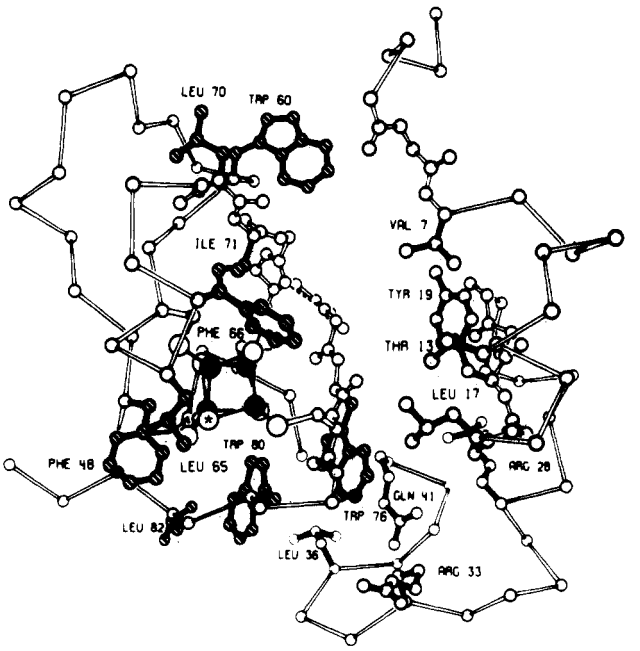

FIGURE 4: Nonpolar contacts in the intramolecular interface. The segment consisting of residues 1–41 is on the *right* and has been separated from the rest of the molecule by translation and rotation. Nonpolar side chains are emphasized by black bonds, and side chains of residues 42–85 are distinguished by striped atoms. The S*4 atom is labeled (*) (Carter et al., 1974a). Reproduced with the permission of The American Society of Biological Chemists, Inc.

When the five species (Tedro et al., 1979) that have been sequenced (*C. vinosum, R. gelatinosa, Thiocapsa pfennigii, Paracoccus* sp., and *Rhodospirillum tenue*) are compared, the Fe_4S_4* cluster is completely buried in a highly hydrophobic cavity with six invariant amino acid side chains (Cys-43, Cys-46, Cys-63, Cys-77, Tyr-19, and Gly-75), and ten hydrophobic residues which are conservatively substituted (Leu-17, Phe-48, Met-49, Leu-65, Phe-66, Gly-68, Ile-71, Trp-76, Trp-80, and Gln-50). Most critically, the X-ray crystallographic work (Carter et al., 1974a,b) shows that the S*2 and particularly the S*4 sulfur atoms (Carter, 1974b) have the closest access to external solvent and are only ~4.5 Å from the surface of the molecule; however, the hydrophobic side chains of Leu-17, Phe-48, Leu-65, Phe-66, and Ser-79 prevent direct contact of these cluster atoms with solvent. Thus, this region in the vicinity of the S*4 atom (see Figure 4) is not only the most accessible region to the redox cluster but also it is the most exposed and accessible hydrophobic region on the protein's surface. With this in mind, it is not unreasonable that the faster rates of TNP-cytochrome *c* result from nonpolar interactions (somewhat akin to binding) between the TNP group–heme crevice and this exposed hydrophobic region. The TNP group would thus facilitate electron transfer by virtue of its hydrophobic properties and would not be acting as an electron bridge.

In terms of molecular topology, the HiPIP reduction mechanism would then possibly include the interaction of and electron transfer in the region of the S*4 sulfur atom. It might be mentioned too that, theoretically, electron transfer takes place with greater facility through hydrophobic (nonpolar) regions of protein than hydrophilic ones (Chance et al., 1979), the reason being that in the theory of electron tunneling the overlap of the wave functions of the redox centers increases as the dielectric constant of the medium decreases. In this context Rawlings et al. (1976) have proposed that the faster rate of oxidation of *C. vinosum* by $Co(phen)^{3+}$ vs. $Fe(CN)_6^{3-}$ was due to the direct attack of the cluster by $Co(phen)^{3+}$

through a hydrophobic region on the HiPIP surface. Although it is at present difficult to distinguish between these and other alternative mechanisms, these reactions probably follow an outer-shere electron-transfer mechanism since there is no evidence that the prosthetic group of either the cytochromes *c* or HiPIP's change their inner sphere of coordination during the reactions.

References

Bartsch, R. G. (1971) *Methods Enzymol. 23*, 644.

Bartsch, R. G. (1978) *Methods Enzymol. 53*, 329.

Brautigan, D. L., Ferguson-Miller, S., & Margoliash, E. (1978) *Methods Enzymol. 53*, 128.

Carter, C. W., Jr., Kraut, J., Freer, S. T., Xuong, N.-H., Alden, R. A., & Bartsch, R. G. (1974a) *J. Biol. Chem. 249*, 4212.

Carter, C. W., Jr., Kraut, J., Freer, S. T., & Alden, R. A. (1974b) *J. Biol. Chem. 249*, 6339.

Chance, B., DeVault, D. C., Frauenfelder, H., Marcus, R. A., Schrieffer, J. R., & Sutin, N., Eds. (1979) *Tunneling Biol. Syst. [Proc. Symp.], 1977*, 614.

De Klerk, H., & Kamen, M. D. (1966) *Biochim. Biophys. Acta 112*, 175.

Dus, K., De Klerk, H., Sletten, K., & Bartsch, R. G. (1967) *Biochim. Biophys. Acta 140*, 291.

Dus, K., Tedro, S., & Bartsch R. G. (1973) *J. Biol. Chem. 248*, 7318.

Feinberg, B. A., & Johnson, W. V. (1980) *Biochem. Biophys. Res. Commun. 93*, 100.

Ferguson-Miller, S., Brautigan, D. L., & Margoliash, E. (1978) *J. Biol. Chem. 253*, 149.

Ilan, Y., Shafferman, A., Feinberg, B. A., & Lau, Y.-K. (1979) *Biochim. Biophys. Acta 548*, 565.

Kortüm, G. (1962) *Kolorimetrie, Photometrie, und Spectrometrie*, p 261, Springer, Berlin.

Marcus, R. A. (1964) *Annu. Rev. Phys. Chem. 15*, 155.

Matthew, J. B., Friend, S. H., Bothelo, L. H., Lehman, L. D., Hanania, G. I. H., & Gurd, F. R. N. (1978) *Biochem. Biophys. Res. Commun. 81*, 416.

Mizrahi, I. A., Wood, F. E., & Cusanovich, M. A. (1976) *Biochemistry 15*, 343.

Osheroff, N. (1979) Ph.D. Thesis, Northwestern University, Evanston, IL.

Osheroff, N., Borden, D., Koppenol, W. H., & Margoliash, E. (1980) *J. Biol. Chem. 255*, 1689.

Perlmutter-Hayman, B. (1971) *Prog. React. Kinet. 6*, 239.

Rawlings, J., Wherland, S., & Gray, H. B. (1976) *J. Am. Chem. Soc. 98*, 2177.

Smith, H. T., Studenmeyer, N., & Millet, F. (1977) *Biochemistry 16*, 4971.

Sokolovsky, M., Riordan, J. R., & Vallee, B. L.(1967) *Biochem. Biophys. Res. Commun. 27*, 20.

Tanford, C. (1961) *Physical Chemistry of Macromolecules*, p 466, Wiley, New York.

Tedro, S. M., Meyer, T. E., & Kamen, M. D. (1976) *J. Biol. Chem. 251*, 129.

Tedro, S. M., Meyer, T. E., & Kamen, M. D. (1979) *J. Biol. Chem. 254*, 1495.

Wada, K., & Okunuki, K. (1969) *J. Biochem. (Tokyo) 66*, 249.

Wherland, S., & Gray, H. B. (1976) *Proc. Natl. Acad. Sci. U.S.A. 73*, 2950.

Biosynthesis of the Macrolide Antibiotic Chlorothricin†

Oreste A. Mascaretti, Ching-jer Chang, Derek Hook, Hideaki Otsuka, Ernest F. Kreutzer, and Heinz G. Floss*

ABSTRACT: Feeding experiments with ^{13}C-labeled precursors followed by ^{13}C NMR analysis of the antibiotic and its aglycon have established a polyketide mode of biosynthesis for chlorothricin, a metabolite of *Streptomyces antibioticus*. The acyl moiety is a substituted 6-methylsalicylic acid derived from four acetate units and a methyl group of methionine. The aglycon is comprised of ten acetate and two propionate units, leaving three carbon atoms, C-22, -23, and -24, unaccounted for. The two 2-deoxy-D-rhamnose moieties are derived from glucose with retention of the hydrogens at C-1, C-2, and C-6 and loss of H-3 and H-5. The hydrogen at C-4 of glucose is transferred intramolecularly to C-6 of the hexose, replacing the hydroxyl group at C-6 in an inversion mode, a result which implicates the thymidine 5′-diphosphate-glucose oxidoreductase reaction in this transformation.

In a previous paper (Holzbach et al., 1978), we presented results pointing to some of the basic building blocks of chlorothricin (I), a novel macrolide antibiotic produced by *Streptomyces antibioticus* strain Tü 99 (Keller-Schierlein et al., 1969; Muntwyler & Keller-Schierlein, 1972; Brufani et al., 1972). These studies had indicated that acetate, propionate, glucose, and methionine were good precursors of the antibiotic and that the latter provides only the *O*-methyl group but none of the *C*-methyl groups of I. In addition, the amino acids tyrosine, phenylalanine, and leucine were fairly well incorporated but not shikimic or mevalonic acid. We now report further results on the mode of incorporation of these precursors into chlorothricin.

Materials and Methods

Radioactive precursors were purchased from Amersham-Searle or from New England Nuclear Corp., except for (6*R*)- and (6*S*)-D-[4-^2H,6-^3H]glucose which had been synthesized

† From the Department of Medicinal Chemistry and Pharmacognosy, School of Pharmacy and Pharmacal Sciences, Purdue University, West Lafayette, Indiana 47907. *Received April 23*, 1980. This work was supported by the U.S. Public Health Service through National Institutes of Health Research Grant AI 11728 (to H.G.F. and C.C.) and Fogarty International Research Fellowship TW 02567 (to O.A.M).

0006-2960/81/0420-0919$01.00/0